Suppression of the Hypoxia-Inducible Factor-1 Response in Cervical Carcinoma Xenografts by Proteasome Inhibitors

Diana C. Birle[1] and David W. Hedley[1,2]

[1]Division of Applied Molecular Oncology, Ontario Cancer Institute and [2]Departments of Medical Oncology and Hematology, Princess Margaret Hospital and University of Toronto, Toronto, Ontario, Canada

Abstract

Experimental data suggest therapeutic advantage from selective disruption of the hypoxia response. We recently found that the proteasome inhibitor bortezomib decreases tumor carbonic anhydrase IX (CAIX) expression in colon cancer patients and herein report a companion laboratory study to test if this effect was the result of hypoxia-inducible factor (HIF) inhibition. Human cervical (SiHa and Me180) and colon (RKO) carcinoma cell lines were treated with bortezomib or the structurally unrelated proteasome inhibitor MG132 in normoxic and hypoxic conditions *in vitro*. Two different *in vivo* experiments investigated bortezomib effects after single dose (2 mg/kg, 24 h) or longer exposure in severe combined immunodeficient mice bearing SiHa xenografts. Treatment with either drug produced accumulation of HIF-1α *in vitro* but strongly inhibited the production of CAIX and vascular endothelial growth factor (VEGF) under hypoxia. This correlated with more than 10-fold reduction in HIF-1 transcriptional activity under hypoxic conditions. A similar effect of bortezomib was seen *in vivo*, using the nitroimidazole probe EF5 to define regions of tumor hypoxia and a triple immunofluorescence technique to measure the spatial distributions of HIF-1α and CAIX. Plasma VEGF levels decreased by ~90% during treatment with bortezomib, indicating that this agent can potently inhibit the hypoxia response in tumors. [Cancer Res 2007;67(4):1735–43]

Introduction

The 26S proteasome is involved in the disassembly of proteins that have been targeted by ubiquitin ligases. In addition to the disposal of proteins that are defective, due for example to misfolding, the ubiquitin ligase/proteasomal system plays an active role in regulating the levels of proteins involved in the control of cell processes, including the regulation of the cell cycle and several transcription factors (1). Because the turnover of many of these proteins in cancers is different from that seen in normal tissues, its disruption by proteasomal inhibition represents a novel and potentially effective approach to cancer treatment (2). This is supported by preclinical data as well as results from early clinical trials using the selective proteasome inhibitor bortezomib (Velcade, formerly known as PS341), which is currently the only proteasome inhibitor tested for anticancer effects in humans (3). Bortezomib has shown activity in several hematologic malignancies and is now approved for the treatment of multiple myeloma patients. Currently, bortezomib is being tested against lymphoma and a range of common solid tumors (2, 3).

It is now recognized that clinical trials of novel agents should include biological markers to determine the drug effects at the molecular level in addition to standard clinical response end points. The cellular content of several important proteins is altered during treatment with proteasome inhibitors. Although it remains uncertain which of these play a significant role in the anticancer action, particular attention has been paid to IκB, a negative regulator of the nuclear factor-κB (NF-κB) transcription factor that seems to play a major role in cancer growth as well as resistance to cytotoxic drugs and radiation. However, there is little direct evidence to show that suppression of NF-κB activation occurs in cancer patients treated with bortezomib, and it is important to consider other potential molecular mechanisms of anticancer effect.

Another important transcription factor that is regulated in a proteasome-dependent manner is hypoxia-inducible factor-1 (HIF-1). Under aerobic conditions, the HIF-1α subunit undergoes proline hydroxylation at Pro^{402} and Pro^{564} that is recognized by von Hippel-Lindau (VHL)–dependent ubiquitin ligases and targeted for proteasomal degradation (4, 5). The proline hydroxylases (PHD) are suppressed under hypoxia, allowing accumulation of HIF-1α, which then associates with its dimerization partner HIF-1β to form the HIF-1 transcription factor. Several transcriptional targets are activated by HIF-1 that in aggregate promote survival under hypoxic conditions. These include enzymes involved in glucose uptake and metabolism, carbonic anhydrase IX (CAIX) that plays a role in the buffering of acidic products of glycolysis, erythropoietin, and vascular endothelial growth factor (VEGF; ref. 6).

It has been shown previously that proteasome inhibition results in the accumulation of HIF-1α in tissue culture under aerobic conditions, although in at least some experimental systems, this is not able to form transcriptionally active HIF-1 heterodimers (7, 8). Nevertheless, because HIF-1 activation promotes cancer cell survival in regions of tumor hypoxia, we considered that HIF-1α accumulation during bortezomib treatment might be a useful biomarker for pharmacodynamic effects in cancer patients. This was tested in a phase II clinical trial of bortezomib in patients with chemotherapy-refractory colorectal cancer metastatic to liver, conducted by the Princess Margaret Hospital Phase II Consortium and reported elsewhere (9). As part of that trial, patients consented to image-guided core biopsies from liver metastases at baseline and after 1 week of treatment with bortezomib. Parallel tissue sections were stained by immunohistochemistry for HIF-1α and the HIF-1 transcriptional product CAIX, and the extent of staining was quantified by digital image analysis of the viable tumor tissue. Unexpectedly, we found a highly significant decrease in the amount of CAIX expression in relation to HIF-1α as well as an overall increase in HIF-1α and decrease in CAIX following treatment with

Note: Supplementary data for this article are available at Cancer Research Online (http://cancerres.aacrjournals.org/).

Requests for reprints: David W. Hedley, Departments of Medical Oncology and Hematology, Princess Margaret Hospital, 610 University Avenue, Toronto, Ontario, Canada M5G 2M9. Phone: 416-946-2262; Fax: 416-946-6546; E-mail: david.hedley@uhn.on.ca.

doi:10.1158/0008-5472.CAN-06-2722

bortezomib, suggesting that in addition to the anticipated increase in HIF-1α, the production of CAIX in hypoxic regions of colon cancer was being disrupted by bortezomib. The possibility that bortezomib was acting to inhibit HIF-1 activity under hypoxic conditions was therefore tested in a companion laboratory study that forms the basis of the present report.

Materials and Methods

Reagents and antibodies. Bortezomib (formerly known as PS341) was obtained from Millenium Pharmaceuticals, Inc. (Cambridge, MA), and MG132 was purchased from Calbiochem (San Diego, CA). Bortezomib used for tissue culture and MG132 were both dissolved in DMSO, aliquoted, and stored at −20°C. The antibodies used were against HIF-1α (BD Biosciences, Mississauga, Ontario, Canada), α-tubulin (Oncogene, Cambridge, MA), β-actin (Abcam, Inc., Cambridge, MA), cleaved caspase-3 (Cell Signaling Technology, Beverly, MA), FIH-1 (Novus Biologicals, Inc., Littleton, CO), p21 (Calbiochem, EMD Biosciences, Inc., San Diego, CA), p53 (Santa Cruz Biotechnology, Inc., Santa Cruz, CA), p84 (Genetex, Inc., San Antonio, TX), and p300 (NH_2 terminus; Santa Cruz Biotechnology), whereas 4′,6-diamidino-2-phenylindole (DAPI) was from Roche Diagnostics (Manheim, Germany). Anti-CAIX and anti–Pro^{564}-HIF-1α antibodies (10, 11) were kind gifts from Dr. A. Harris (University of Oxford, Oxford, United Kingdom), whereas anti-EF5 was from Dr. Cameron Koch (University of Pennsylvania, Philadelphia, PA). The secondary antibodies for indirect immunofluorescence staining were Cy-3–conjugated donkey anti-rabbit and Cy-5–conjugated antimouse (Jackson ImmunoResearch, West Grove, PA), whereas the ones used for Western blots (antimouse and antirabbit IgG antibodies) were from Amersham Biosciences (Buckinghamshire, United Kingdom). Protein G-Sepharose was from Sigma-Aldrich Canada Ltd. (Oakville, Ontario, Canada).

Cell culture. The human cervical squamous cell carcinoma SiHa and Me180, colon carcinoma RKO, and prostate carcinoma PC3 cell lines were obtained from American Type Culture Collection (Manassas, VA). SiHa was grown in α-MEM, Me180 in McCoy's medium, RKO in Ham's F-12:DMEM H21 1:1, and PC3 in Ham's/F-12 medium. All the media for cell culture were supplemented with 10% fetal bovine serum, and cells were grown at 37°C and 5% CO_2 in air, unless otherwise specified.

Cell treatment, cellular fractionation, immunoprecipitation, and immunoblotting. Cells grown at 60% to 70% confluence were treated with proteasome inhibitors and exposed to normal atmosphere (21% O_2, 5% CO_2, balance air) or low (0.2% O_2, 5% CO_2, balance nitrogen) O_2 concentrations in sealed, humidified chambers (Modular Hypoxia Chambers, Billups-Rothenberg, Inc., Del Mar, CA). After 24 h, the cells were processed to obtain a total lysate [50 mmol/L HEPES (pH 8.0), 10% glycerol, 1% Triton X-100, 150 mmol/L NaCl, 1 mmol/L EDTA, 1.5 mmol/L $MgCl_2$, 100 mmol/L NaF, and 10 mmol/L NaP_2O_7 supplemented with 1 mmol/L Na_3VO_4 and protease inhibitor cocktail (Roche Diagnostics)] or separate cytoplasmic fraction [15 min of incubation with Dignam buffer: 10 mmol/L HEPES-NaOH (pH 7.9), 1.5 mmol/L $MgCl_2$, 10 mmol/L KCl, 0.5 mmol/L DTT, 0.5 mmol/L phenylmethylsulfonyl fluoride (PMSF), 0.1% NP40, 1 mmol/L Na_3VO_4, protease inhibitor cocktail; spun for 5 min] and nuclear fraction [30 min of incubation with extraction buffer: 10 mmol/L HEPES (pH 7.4), 422 mmol/L NaCl, 2 mmol/L EDTA, 0.1 mmol/L DTT, 200 μmol/L PMSF, 1 mmol/L Na_3VO_4, protease inhibitor cocktail]. For immunoprecipitation, cleared lysates were precipitated with anti-FIH antibody and collected on Protein G-Sepharose. Equivalent amounts of protein (assayed with bicinchoninic acid protein assay from Pierce PerBio, Rockford, IL) were separated by 7.5% or 10% SDS-PAGE gels. Proteins were transferred to polyvinylidene difluoride membranes (Millipore, Bedford, MA) and probed with the appropriate antibodies according to the manufacturer's instructions. Detection was conducted using enhanced chemiluminescence (ECL) or ECL Plus chemiluminescence kits (Amersham Biosciences).

For the irradiation experiment, whole-cell ionizing radiation using a ^{137}Cs irradiator (MDS Nordion, Ottawa, Ontario, Canada) at 1 Gy/min (room temperature, aerobic conditions) was done on SiHa cells.

Luciferase assays. The constructs used for cotransfections were kind gifts from other laboratories: 5× hypoxia response element (HRE)-luciferase (5× HRE-luc) from Dr. A. Giaccia (Stanford University, Stanford, CA), and the control plasmid lacking the HREs cytomegalovirus-luciferase (CMV-luc) from Dr. R. Hill (University of Toronto, Toronto, Ontario, Canada). The pcDNA3.1/His/LacZ was obtained from Invitrogen (Carlsbad, CA). Transfection was done using Fugene 6 (Promega, Madison, WI) according to the manufacturer's instructions. On the 2nd day, after cotransfections, cells were reseeded, and the next day, drug treatment together with exposure to normoxic or hypoxic conditions began. After 24 h of treatment, cells were lysed, and the luciferase assay was completed according to the manufacturer's instructions (Dual-Light System, A&B Biosciences, Bedford, MA). The results were normalized to the values read for β-galactosidase activity. The luminometer used was Luminoskan Ascent (ThermoLab Systems, Franklin, MA).

SiHa xenografts. Animal experiments were done in the Animal Facility of the Princess Margaret Hospital, operated under the guidelines approved by the Canadian Council for Animal Care. SiHa cell suspension (0.1 mL; containing approximately 5×10^5 cells) was injected into the left gastrocnemius muscle of severe combined immunodeficient (SCID) mice. After ~3 weeks, the tumors became readily visible and the tumor + leg diameter measured between 10 to 11 mm (tumor mass, ~0.4 g). The clinical formulation of bortezomib, made up freshly each day, was used for these experiments. Two *in vivo* experiments were done: one to investigate the acute effect of bortezomib (2 mg/kg i.p. single dose) and another one to assess the effects of a prolonged treatment (up to three doses of 1.5 mg/kg i.p. every other day). In the first experiment, 8 mice were randomly assigned to bortezomib or drug vehicle control, whereas in the second, 20 mice were assigned to four groups: single dose, two doses, and three doses of bortezomib or three doses for vehicle control. Mice were killed 24 h after the last treatment, blood samples were obtained by cardiac puncture, and the tumors were excised. Four hours before killing, the nitroimidazole hypoxia probe EF5 was injected both i.p. and i.v. Each tumor was dissected from the surrounding tissues and cut into several slices: some were snap frozen in liquid nitrogen, and the rest were fixed in formalin for 24 h and paraffin embedded. The blood was collected in heparin-coated syringes and centrifuged at low speed, and the supernatant was frozen at −70°C. The VEGF ELISA assay was done according to the manufacturer's instructions (R&D Systems, Minneapolis, MN). This kit recognizes both human $VEGF_{165}$ and $VEGF_{121}$ and at 50 ng/mL does not cross-react with mouse VEGF.

Immunofluorescence staining. Serial sections were cut from ornithine carbamyl transferase–embedded tumor tissue: one of them was stained with H&E for transmitted light microscopy and used for selecting the tumoral areas, on which the further image analysis was to be done. The other sections were multiple labeled for the following: (*a*) HIF-1α, CAIX, and EF5 and (*b*) HIF-1α and cleaved caspase-3. Secondary antibodies used alone were control for nonspecific background. All sections were counterstained with DAPI 1μg/mL to outline the nuclear area. Measurements of stained area were made only in the viable tumor areas excluding necrotic or non tumoral tissue.

Computerized image analysis. Tissue sections were examined using a Microcomputer Imaging Device image analysis system (Imaging Research, Inc., St. Catharines, Ontario, Canada) equipped with a Quantix cooled CCD camera (Photometrics, Tucson, AZ) mounted on an Olympus BX50 epifluorescence microscope. The analysis included the entire viable tumoral area identified on the slide, using a scanning autostage to create composite images of individual fields at ×20 magnification as described previously (12). A tumoral map that included only viable tumor was made using the H&E sections and then carefully adjusted on the composite DAPI images. The final image analysis was done using in-house developed software written in IDL 6.1 (Research Systems, Inc., Boulder, CO). For the 12-bit grayscale images, the threshold was set individually at a brightness level that best separated the signal from the background. For each marker, we measured the percentage of positive stained area, based on the threshold images. Only the part of the image that corresponded to the tumoral map was analyzed.

Statistical analysis. The *in vitro* experiments were done at least thrice and representative results are shown. Statistical analysis was done using SigmaStat 2.0 (SPSS Science, Chicago, IL). Differences in protein expression between *in vivo* treatment groups was assessed using Student's *t* test for normally distributed data or the Mann-Whitney rank-sum test for nonnormally distributed data. $P < 0.05$ was used as the cutoff for statistical significance.

Results

In vitro Experiments

Effects of proteasome inhibitors on accumulation of HIF-1α and inhibition of CAIX and VEGF expression during hypoxia. SiHa and Me180 (cervical carcinoma cell lines) and RKO (colon carcinoma) were treated for 24 h with bortezomib or the structurally unrelated proteasome inhibitor MG132 and exposed during this interval to either normal (21%) or low (0.2%) oxygen concentrations. Whole lysates were used for Western blotting (Fig. 1*A* and *B, SiHa*; *C, Me180*; and *D, RKO*), whereas secreted VEGF levels were measured in the medium collected from the SiHa-treated samples (Fig. 1*E*). Bortezomib and MG132 protected the HIF-1α subunit from proteasome degradation and, as expected, the protein accumulated in aerobic as well as in hypoxic conditions. Concurrently, the expression of CAIX and VEGF, which is HIF dependent, was suppressed under hypoxia. The increased expression of HIF-1α under aerobic conditions was not associated with the expression of CAIX or change in VEGF levels when compared with the control, suggesting that the function of HIF-1α was impaired by the proteasome inhibitors, regardless of oxygen tension.

Proteasome inhibitors negatively affect HRE transcription. SiHa cervical carcinoma and RKO colon carcinoma cells were transfected with different luciferase constructs: either one containing five HRE inserts (5× HRE-luc) or one lacking any HRE sequence (CMV-luc) as a control for the hypoxic response and a β-galactosidase reporter to normalize the luciferase readings. The cells were treated with proteasome inhibitors for 24 h while exposed to either aerobic or hypoxic conditions. Hypoxia-induced HRE binding–dependent transcription for SiHa cells was more than 400-fold higher in untreated cells when compared with normoxia. As shown in Fig. 1*F*, in SiHa cells, bortezomib and MG132 inhibited this in a dose-dependent manner. Because RKO cells were more sensitive to the drugs, lower concentrations were used to avoid excessive cellular death; at 50 nmol/L bortezomib, the transcription was almost completely suppressed (Fig. 1*G*).

Proteasome inhibitors induce nuclear accumulation of HIF-1α. Several reports using confocal microscopy addressed previously the cellular localization of HIF-1α during inhibition of proteasomal degradation, but with conflicting results. Although some suggested that this type of treatment might affect transcriptional activity of HIF-1α as the nuclear translocation of the molecule is impaired (7), others found that, in normoxia, on addition of MG132, HIF-1α is located within the nucleus, although with a distinct punctuate pattern (13). In our case, cellular fractionation of SiHa cells treated with proteasome inhibitors showed that under both aerobic and hypoxic conditions, HIF-1α is found predominantly in the nucleus (Supplementary Fig. S1).

Effect of proteasomal inhibition and hypoxia on HIF-1α interaction with prolyl hydroxylases and FIH-1. Because the proteasome can also regulate the cellular levels of prolyl hydroxylases (14), we considered that their accumulation during treatment with proteasome inhibitors might contribute further to modifying the hypoxia response. As shown in Fig. 2*A*, under normoxic conditions, treatment of SiHa cells with bortezomib resulted in accumulation of the hydroxylated form of HIF-1α (at Pro^{564}), consistent with the accepted role of the proteasome in HIF-1α degradation under these conditions (7). However, we also observed accumulation of hydroxylated HIF-1α at low oxygen levels that was markedly increased in the presence of proteasome inhibitors, suggesting the persistence of some PHD activity under hypoxia.

FIH-1 is another enzyme responsible for HIF-1α hydroxylation (Asn^{803}) and also for subsequent impaired function of HIF, as this inhibits binding to the transcriptional coactivator p300 (5). To test if HIF-1α accumulated during proteasome inhibition associated with FIH-1, we did immunoprecipitation with the respective antibody on lysates from SiHa cells treated with bortezomib or MG132 for 24 h under normoxic conditions or 0.2% O_2. As shown in Fig. 2*B*, both drugs increased the levels of HIF-1α complexed with FIH-1, and this effect was seen under hypoxic as well as aerobic conditions.

Previous studies favored cytoplasmic localization for FIH-1 (5), whereas others reported significant amount in the nucleus (15). Although we showed the presence of HIF-1α–FIH-1 complex, because HIF-1α was found mostly in the nucleus, we were interested in investigating FIH-1 access to its substrate. As shown in Fig. 2*C*, FIH-1 was indeed mainly cytoplasmic; however, there was also a certain nuclear amount. Of interest, exclusively in the nuclear fraction, we noticed a strong band slightly above 120 kDa. This was identified using FIH-1 antibodies from two different sources. Additionally, excessive stabilization of FIH-1 when the proteasome is inhibited or under hypoxia can be excluded because the protein level was basically constant regardless the treatment or oxygen concentrations (Fig. 2*D*).

Both types of hydroxylases (PHDs and FIH-1) remain active in low-oxygen conditions as was shown by our results, whereas PHDs are reported to accumulate when proteasomal degradation is inhibited (14). Hydroxylation of HIF-1α at Pro^{564} and Pro^{402} provides a much higher affinity for VHL, which ensures further ubiquitination and recruitment of corepressors, whereas hydroxylation at Asn^{803} impairs the binding of transcription coactivators (16–18). Thus, we considered that modification of these enzymes might explain the loss of transcription with bortezomib.

Cobalt is a well-known inhibitor of hydroxylases, and FIH-1 is reported to be more sensitive than PHDs (19). However, similar to the effects seen with hypoxia, treatment with the bortezomib and MG132 inhibited the activation of CAIX when SiHa cells were treated with 100 μmol/L $CoCl_2$ for 24 h (Fig. 2*E*).

p53 and HIF-1α during proteasomal inhibition. There is an important body of literature describing the relationship between p53 and HIF-1α during hypoxia, mediated or not through Mdm2. p53 is reported to participate in HIF-1α degradation (20–23) as well as in inhibition of HIF transcriptional function through competition for the coactivator p300 (22). The cellular levels of p53 are also adjusted by the proteasome, and treatment with bortezomib or MG132 resulted in the accumulation of p53 in SiHa and Me180 cells (Fig. 3*A* and *B*). To test if p53 was transcriptionally active following treatment with proteasome inhibitors, we measured the expression of p21 following exposure to hypoxia or irradiation and found that this was not suppressed by bortezomib or MG132 (Fig. 3*A* and *B*). These results suggest that the inhibition of HIF-1 is not simply due to nonspecific effects of proteasome inhibition on transcription. Note that both of these cell lines express the E6 papilloma viral

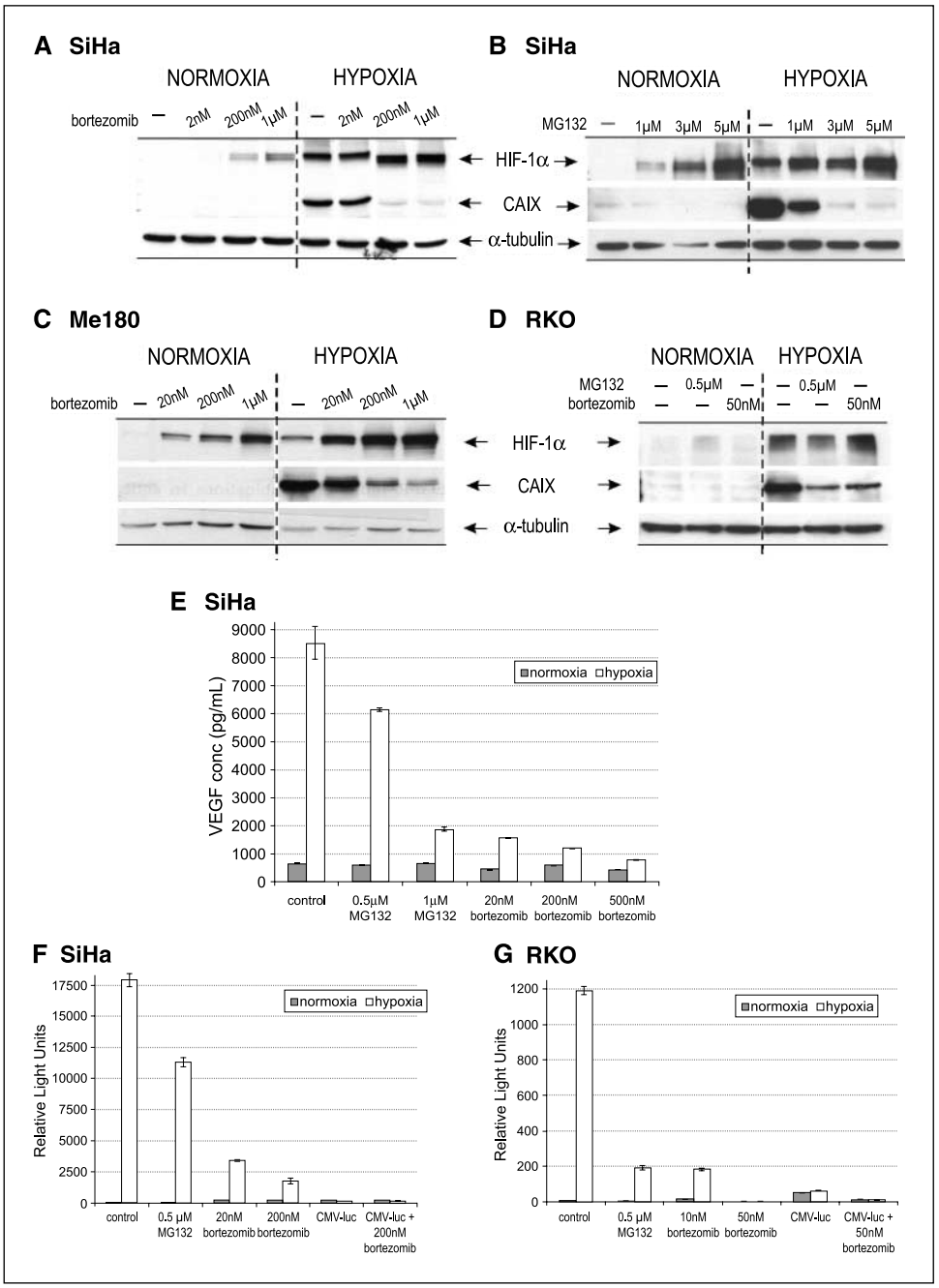

Figure 1. Treatment of human epithelial cancer cells with proteasome inhibitors bortezomib and MG132 results in accumulation of HIF-1α and suppression of CAIX and VEGF expression. Western blotting of whole lysate for SiHa (*A* and *B*) and Me180 (*C*) cervical carcinoma cells and for RKO (*D*) colon cancer cells treated with bortezomib and MG132, respectively, and exposed to either normal (21%) or low (0.2%) oxygen concentrations for 24 h. *E,* ELISA assay for VEGF secreted by SiHa cells treated with both drugs and exposed to normoxia or hypoxia for 24 h. All these experiments were done at least thrice. Representative results are shown. The ELISA assays were done in triplicate. Treatment with bortezomib inhibits HRE-driven transcription in SiHa (*F*) and RKO (*G*) cells under hypoxic conditions. CMV-luc construct lacks the HREs and was used as a control for the hypoxia response. Luciferase values were normalized to the readings for β-galactosidase. These experiments were done in triplicate. *Columns,* mean; *bars,* SD. Experiments were done at least thrice. Representative results are shown.

protein that accelerates p53 degradation, and this probably accounts for the lack of p21 induction by radiation in the absence of proteasome inhibition (24).

Because p53 accumulates with proteasome inhibitors and remains functional, consistent with previous reports (24, 25), we considered that this might affect HIF transcription. We tested this using PC3, a prostate carcinoma cell line that is p53 null (26). As shown in Fig. 3*C*, these cells expressed CAIX under aerobic as well as hypoxic conditions, and this was suppressed by the proteasome inhibitors, suggesting that the accumulation of p53 is unlikely to explain the effects of bortezomib on HIF-1 activity.

Proteasome inhibition decreases p300 binding to HIF-1α during hypoxia. In hypoxic conditions, HIF-1 transactivation relies on the recruitment of various coactivators, including p300 that interacts with the HIF-1α COOH terminus to ensure further binding to DNA and transcriptional activation (5). It has been reported previously that DNA binding is maintained during proteasome inhibition (7). To test this, nuclear fractions from SiHa cells were immunoprecipitated with a p300 antibody directed against its NH_2 terminus and probed with an anti–HIF-1α antibody. As shown in Fig. 4, treatment with proteasome inhibitors resulted in decreased binding of HIF-1α to p300 under hypoxia (Fig. 4*A*), with no change in the total cellular levels of p300 (Fig. 4*B*).

In vivo Experiments

Effects of bortezomib on HIF-1α and CAIX in relation to tumor hypoxia. Two groups of four SCID mice bearing i.m. SiHa

xenografts were treated with a single i.p. injection of 2 mg/kg bortezomib or vehicle control. Four hours before sacrifice, animals were treated with the nitroimidazole hypoxia probe EF5, and tumors were harvested at 24 h. As shown in Fig. 5*A*, HIF-1α and CAIX were strongly colocalized with EF5 in control tumors. However, 24 h after bortezomib treatment, there was increased expression of HIF-1α in EF5-negative tissue and a pronounced decrease in the level of CAIX in hypoxic regions: similar to the results seen when SiHa cells were treated with bortezomib and exposed to hypoxia *in vitro* (Fig. 1*A*). The effects on HIF-1α were analyzed by imaging the entire histologic section, manually outlining viable tumoral areas, and then obtaining the percentage of nuclear area (defined by DAPI staining) that was positively labeled for HIF-1α in EF5-negative or EF5-positive regions. As shown in Fig. 5*B*, treatment with bortezomib resulted in statistically significant increases in HIF-1α levels in both the total and the EF5-negative tumoral areas (P_a = 0.012 and P_b = 0.015). The analysis of CAIX did not take into account DAPI staining because this is predominantly a surface membrane protein. As shown in Fig. 5*C*, bortezomib treatment resulted in highly significant decreases in CAIX levels in hypoxic regions defined by EF5 as well as in the HIF-1α–positive and the total viable tumoral areas ($P < 0.001$ in all cases).

Activation of caspase-3 by bortezomib in SiHa xenografts. Because HIF-1–dependent transcription can promote cell survival in hypoxic conditions (27), we asked if bortezomib treatment might enhance apoptosis in hypoxic regions of SiHa xenografts. A total of 20 SCID mice bearing SiHa xenografts were divided into four groups of five each and treated on alternate days with one, two, or three doses of 1.5 mg/kg bortezomib or vehicle control. Animals were injected with EF5 4 h before sacrifice, and the tumors were harvested 24 h after the last bortezomib treatment. Tissue sections were stained for EF5, HIF-1α, and cleaved caspase-3. As shown in Fig. 6, there was an overall increase in the mean percentage tumoral area of cleaved caspase-3 expression after a single dose of bortezomib (4.00 ± 0.72 SE versus 1.51 ± 0.29 SE for control). This

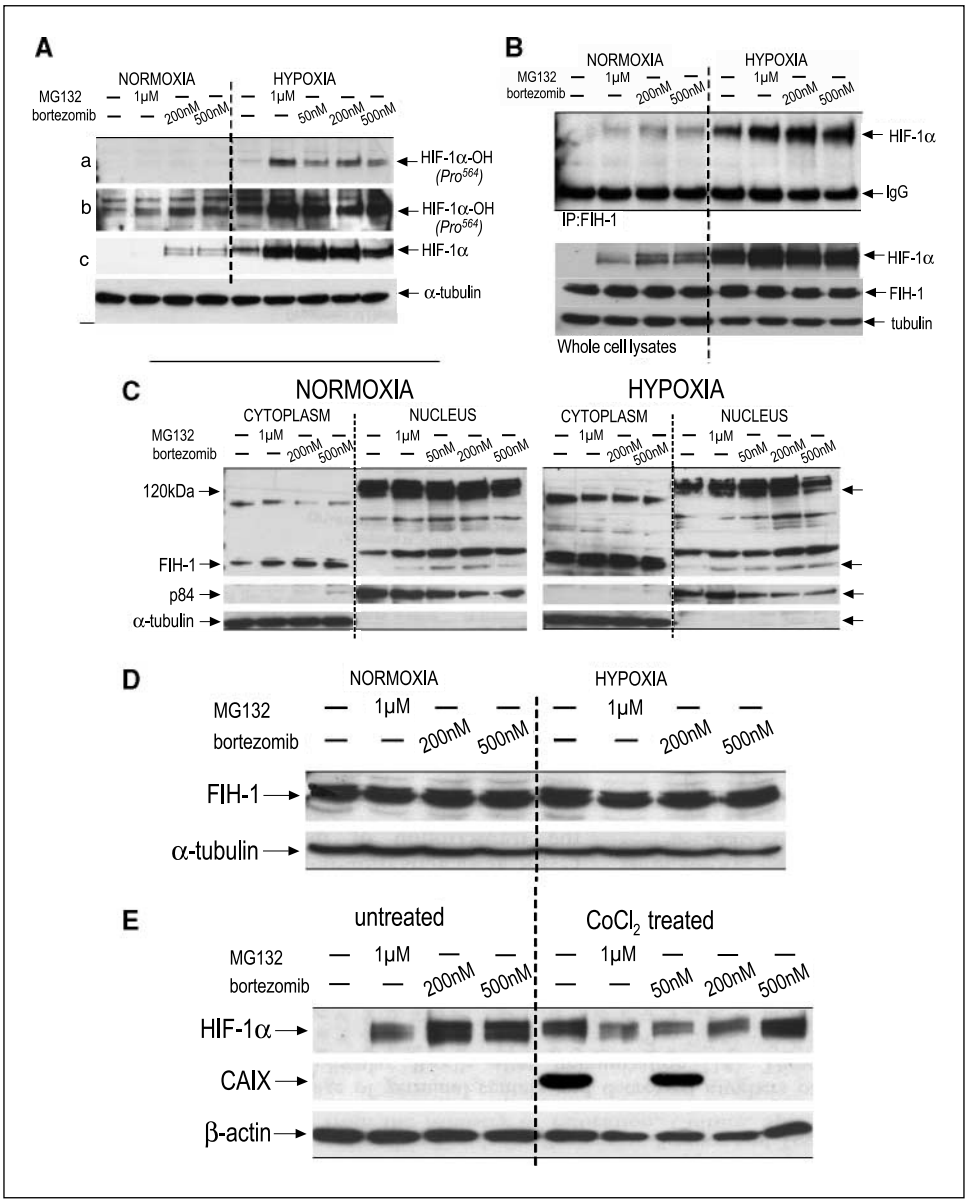

Figure 2. *A,* hydroxylated HIF-1α (*Pro*^{564}) accumulates in SiHa cervical carcinoma cells exposed to normal oxygen concentration or hypoxia (0.2% oxygen) and bortezomib or MG132. The same membrane was exposed for 30 s (*a*) and then 30 min (*b*) using ECL Plus; α-tubulin and HIF-1α reprobing (*c*) served as control. Blots are representative of triplicate experiments. *B,* increasing levels of HIF-1α are complexed with FIH-1 when SiHa cells are treated with proteasome inhibitors and exposed to hypoxia, showing that FIH-1 still binds HIF-1α under hypoxic conditions. Total lysates were immunoprecipitated (*IP*) with anti–FIH-1 antibody, and the blot was probed with anti–HIF-1α antibody. Levels of total HIF-1α and FIH-1 in the cellular lysates used for immunoprecipitation. These results are representative of three independent experiments. *C,* FIH-1 was found mainly in the cytoplasm of SiHa cells, with some nuclear presence and strong signal from a nuclear band heavier than 120 kDa. p84 protein was used as a loading control for the nuclear fraction and α-tubulin for the cytoplasmic fraction. These experiments were done at least thrice. Representative results are shown. *D,* FIH-1 levels are not affected by proteasome inhibition or variation in oxygen concentration (SiHa). *E,* SiHa cells were treated for 24 h with bortezomib or MG132, and $CoCl_2$ (100 μmol/L). Total lysates were blotted and probed with CAIX. All these experiments were done at least thrice. Representative results are shown.

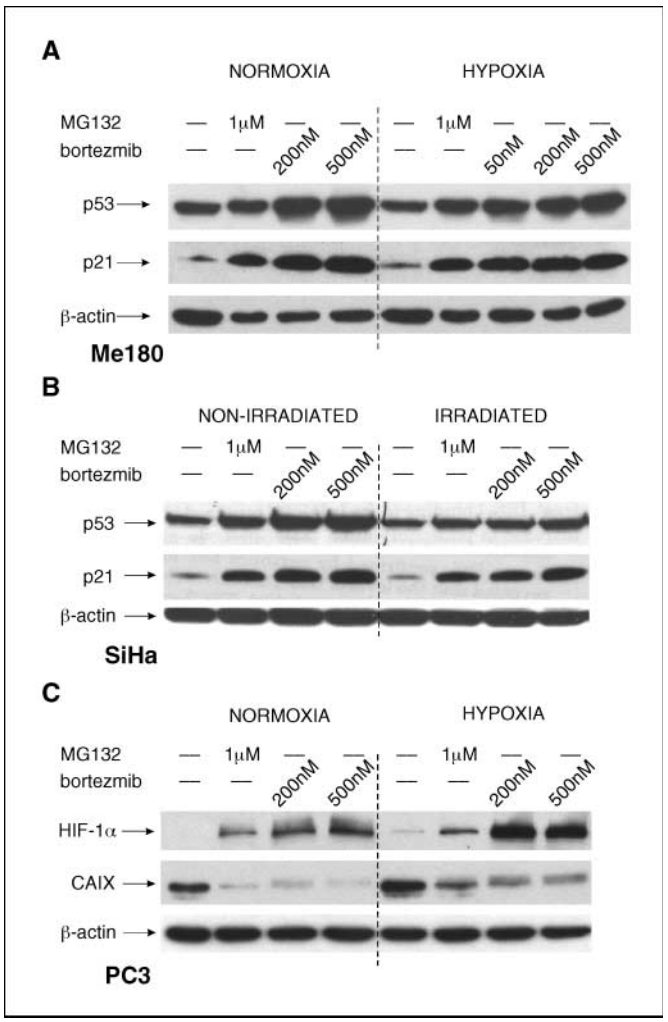

Figure 3. *A,* p53 and p21 accumulated in Me180 cells when treated with bortezomib and MG132, respectively, and exposed to either normal (21%) or low (0.2%) oxygen concentrations for 24 h. *B,* SiHa cells were treated with proteasome inhibitors and irradiated (10 Gy); 6 h later, the cells were collected and total lysates were used for Western blotting. *C,* PC3 prostate carcinoma cells ($p53^{-/-}$) were treated with bortezomib and MG132, respectively, and exposed to either normoxic or hypoxic conditions for 24 h. Total lysates were used for Western blotting. All these experiments were done at least thrice. Representative results are shown.

indicates that the drug has an anticancer effect in this model, although there was no significant effect on tumor volume during the treatment period used in this experiment. When caspase-3 activation was examined in relation to EF5 staining, a pronounced increase was seen in the hypoxic regions of control tumors, relative to the nonhypoxic regions. Significant differences were observed in the time course of caspase-3 activation following bortezomib treatment, which reached a peak after the first injection in the nonhypoxic regions, but only after the second dose in the hypoxic regions.

Bortezomib suppresses plasma VEGF levels in mice bearing SiHa xenograft. Plasma levels of human VEGF were measured in animals treated with 1.5 mg/kg bortezomib, using an ELISA assay. Mean plasma VEGF in untreated control mice was 130.9 ± 31.9 pg/mL SE, and this showed a large decrease 24 h following a single dose of bortezomib, which persisted with alternate day treatment 8.8 ± 3.1 after one dose, 8.7 ± 1.2 after two doses, and 16.7 ± 9.1 after three doses (Supplementary Fig. S2). Because the tumor size was not significantly affected by the drug, this effect is most likely due to the suppressed transcription of the gene.

Discussion

In this report, we show that bortezomib suppresses the activation of HREs and the production of CAIX and VEGF under hypoxic growth conditions *in vitro*, with almost complete inhibition at the highest dose tested. This effect was seen in several human epithelial cancer cell lines and also with the structurally unrelated proteasome inhibitor MG132, suggesting that it might be a general effect of proteasome inhibition in human cancers under hypoxic conditions. Similarly, using the extrinsic nitroimidazole probe EF5 to outline hypoxic microregions of SiHa cervical carcinoma xenografts, we found accumulation of HIF-1α, together with a large decrease in CAIX in hypoxic regions following bortezomib treatment. This effect is consistent with our recent findings in colon cancer patients treated with bortezomib, where there was a significant increase in HIF-1α relative to CAIX in sequential biopsies obtained from liver metastases before and after 1 week of bortezomib (9). Moreover, treatment with bortezomib resulted in a large decrease in the plasma concentration of human VEGF in mice bearing SiHa xenografts, further supporting the idea that this agent is a potent inhibitor of the hypoxic response in solid tumors.

Rapid degradation of the ubiquitinated HIF-1α is considered the principal mechanism through which HIF-dependent transcription is suppressed during normoxia. Because proteasome inhibition *in vitro* produced accumulation of HIF-1α, this was expected to result in the transcription of hypoxia-induced genes, regardless of oxygen level, rather than the observed inhibition of HIF-1, especially under hypoxia. Nevertheless, a "paradoxical" effect of bortezomib on the HIF pathway (28) is already mentioned in the literature, as

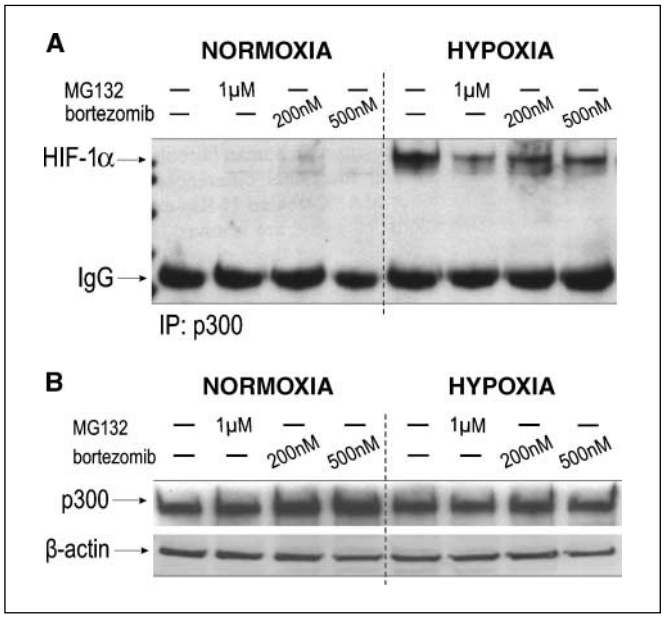

Figure 4. *A,* nuclear fractions from lysed SiHa cells treated with proteasome inhibitors in normoxic and hypoxic conditions were immunoprecipitated with anti-p300 (NH_2 terminus) antibody, and the blot was probed with HIF-1α. *B,* Western blot of total lysates from treated SiHa cells probed with the same p300 antibody. All these experiments were done more than thrice. Representative results are shown.

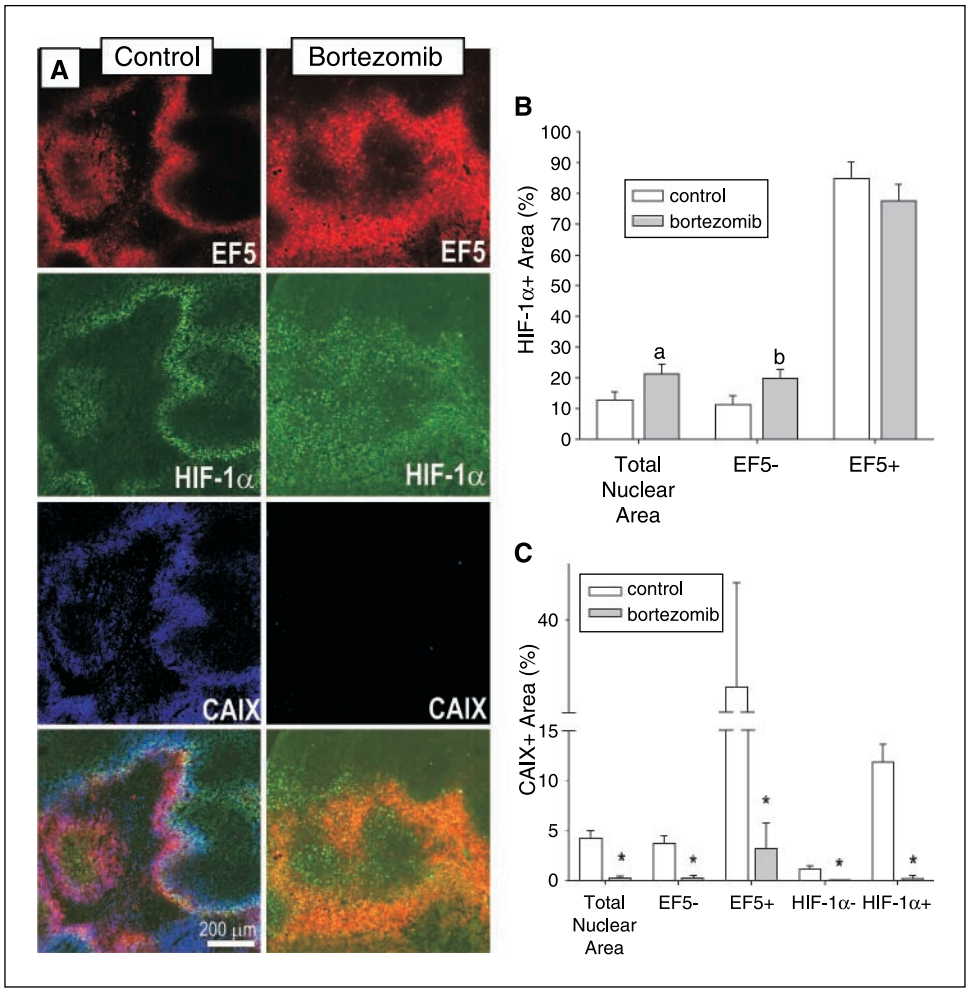

Figure 5. Treatment of mice bearing SiHa xenografts with bortezomib results in both the accumulation of nuclear HIF-1α in nonhypoxic areas and the suppression of CAIX expression. *A,* representative examples of tiled images (1 mm^2 tumoral area at ×200 magnification) from control and bortezomib-treated mice, stained for EF5, HIF-1 α, and CAIX. *B,* analysis of nuclear HIF-1α levels in the total viable tumor area and in nonhypoxic or hypoxic areas defined by EF5 staining (P_a = 0.012 and P_b = 0.015). *C,* effects of bortezomib on CAIX staining in the total viable tumor area and in areas defined by either EF5 or HIF-1α staining (P < 0.001 in all cases). *Columns,* mean of five tumors in each group; *bars,* SE. *a* and *b,* statistical significance when compared with the control. Results from this experiment were shown in McKay et al. (9).

several groups reported an antiangiogenic affect or enhanced apoptosis following *in vivo* treatment with bortezomib, alone or in combination with chemotherapeutic agents (29–31). These observations are in accord with our own findings about VEGF and caspase-3 expression in the described cervical carcinoma *in vivo* model.

An increasing number of studies focused recently on HIF-1α regulation by prolyl hydroxylation. The inhibition of PHDs activity due to decreased oxygen levels is considered critical for HIF-1α escaping from proteasome degradation during hypoxia because the affinity of VHL for the nonhydroxylated HIF-1α is much lower (32–37). However, this concept seems to need adjustment as an overall increase in cellular hydroxylase activity has been observed during hypoxia (38), and there is evidence for the presence of at least some PHD activities in such conditions (37, 39, 40). This is supported by the hypoxic induction of PHD2 and PHD3 transcription (33, 38, 41–43) and also by the elegant study of Appelhoff et al. (40) who showed that it is the abundance of the enzyme that dictates further the involvement of each PHD in HIF regulation. Recently described elements, such as Siah1a/2 and OS-9, might contribute also to this picture. Siah1a/2 are members of the E3 ubiquitin ligase family, efficient within a large range of O_2 concentrations, which can limit PHD1/PHD3 amounts during hypoxia by mediating their proteasomal degradation (14). Ubiquitously expressed OS-9 binds to both HIF-1α and PHDs and can further enhance hydroxylases activity (44).

Consequently, it was attractive to consider prolyl-hydroxylases of importance when examining the effect of bortezomib on HIF activity. Protected from proteasomal degradation, PHDs might accumulate, particularly during hypoxia when their transcription is induced, resulting in the higher levels of hydroxylated HIF-1α shown in Fig. 2*A*. Hydroxylation at Pro^{402}/Pro^{564} seems to be an irreversible process (39, 40) and increases pVHL affinity for HIF-1α by several orders of magnitude (17, 18, 45). This leads to further poly-ubiquitination, recruitment of transcriptional corepressors (histone deacetylases), and impaired HIF function (16).

Although HIF-1α accumulates during hypoxia, additional regulatory steps are required to fine-tune its activity. FIH-1 (the inhibiting factor of HIF-1) is an asparaginyl hydroxylase that binds to the HIF-1α–VHL complex> and controls HIF-1 transactivation by obstructing the recruitment of CBP/p300 coactivators (16, 36, 46). Of interest, FIH-1 is functionally active in both aerobic and hypoxic conditions (16, 47), consistent with the coprecipitation data shown in Fig. 2*B*. Our data indicate also that PHDs activity and the binding of FIH-1 to HIF-1α are maintained in the presence of bortezomib, regardless of the oxygen concentration, whereas, in contrast with PHDs accumulation during proteasome inhibition (14), FIH-1 levels are not modified (Fig. 2*D*). Furthermore, the effects of proteasome inhibition on HIF function were similar in hypoxia and when HIF-1α was induced using cobalt. Because cobalt mimics hypoxia by inhibiting both PHDs and FIH-1 (19), we

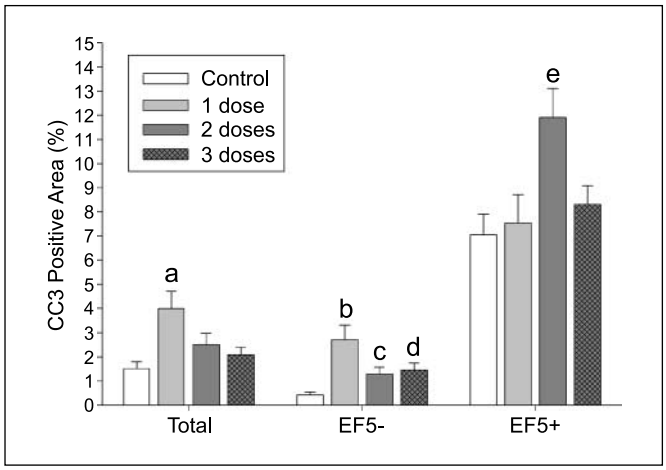

Figure 6. Treatment of mice bearing SiHa xenografts with bortezomib induces a significant apoptotic response after the first or second dose in EF5-negative and EF5-positive areas, respectively. The percentage of positive staining for cleaved caspase-3 (*CC3*) is reported to the total tumoral area and hypoxic and nonhypoxic areas. *Columns,* cleaved caspase-3–positive area; *bars,* SE. *a* to *e*, $P_a = 0.002$, $P_b < 0.001$, $P_c = 0.007$, $P_d < 0.001$, and $P_e = 0.01$, statistical significance when compared with the control.

conclude from these results that PHD and FIH-1 activity is not essential for the suppression of HIF-1 by proteasome inhibitors. Moreover, because increased binding of HIF-1α to VHL in the absence of hydroxylation is unlikely, it cannot explain the treatment effect.

We next investigated effects of bortezomib on p53 function because this is regulated also by proteasomal degradation and can interfere with HIF-1–driven transcription. However, in PC3 $p53^{-/-}$ prostate cancer cells, we obtained similar inhibition of HIF-1 by bortezomib as in the other cell lines (Fig. 3). Furthermore, although bortezomib induced its accumulation in SiHa and Me180 cells, p53 remained functional as shown by p21 induction by hypoxia or irradiation. Thus, we conclude that the effect on HIF-1α is independent of the p53 status and, in contrast with a previous report (7), it cannot be explained by nonselective suppression of transcription by proteasome inhibitors.

Demidenko et al. (48) described a self-limiting mechanism whereby HIF-1α transcriptionally induces its own degradation during hypoxia. Consequently, transcription inhibition at low oxygen levels leads to a "super induction" of HIF-1α that could explain the more increased accumulation of HIF-1α protein in hypoxia versus normoxia following bortezomib treatment. These reports, as well as our own data, reemphasize the differential regulation of HIF-1α in hypoxia versus normoxia. Aside from the HIF-1 transcriptional self-limiting loop, p53, and PHDs, other molecules were found to alter HIF-1α, also only at specific times and to a certain extent. For example, normal oxygen concentrations are optimal for ARD1, critical for HIF-1α binding by VHL (47), whereas a hypoxic environment ensures the activity of thioredoxin, which contributes to HIF-1 transactivation together with Ref-1 (49).

At the present time, the mechanism by which proteasome inhibitors suppress the response to hypoxia remains unclear. Based on our results, we can conclude that this is a specific effect toward HIF-1α and exclude prolyl and asparaginyl hydroxylases as well as p53 as determinant factors. Nevertheless, alterations involving other molecules that interact with HIF-1α, whether they are positive or negative regulators, or conformational modifications of HIF-1α molecule itself, could lead to this outcome, as we were able to show lower binding of the p300 transcriptional coactivator. It should be noted that shortly after this article was submitted, Kaluz et al. (50) also reported that bortezomib disrupts the transcriptional activity of HIF-1α via specific effects on the COOH-terminal activation domain and that this effect was relieved by overexpressing p300. Unlike our findings, these authors were not able to show decreased p300 binding following proteasome inhibition. However, because our own immunoprecipitation data (Fig. 4*A*) show only partial loss of HIF-1α binding, which might be explained by differences in experimental technique, we would agree with Kaluz et al. that the direct inhibition of p300 interaction is not sufficient to explain the profound loss of HIF-1α transcriptional activity under proteosome inhibition.

Tumor hypoxia is an adverse prognostic feature in human cancers, and hypoxic tumors are less sensitive to cancer treatments, such as chemotherapy and radiation. Experimental results suggest that agents targeting HIF-1 might be selectively toxic to hypoxic tumor tissue and therefore enhance the effects of conventional therapy. Together with the recent article by Kaluz et al. (50), we believe that the results shown here provide a mechanistic explanation for our earlier empirical finding that bortezomib treatment disrupts the hypoxia response in the liver metastases of colorectal cancer patients (9). Further investigation of an anti–HIF-1 role for bortezomib, and probably other proteasome inhibitors, should include preclinical testing of combinations with radiation treatment and additional pharmacodynamic measurements, such as plasma VEGF levels, aimed to detect HIF-1 inhibition effects in human clinical trials.

Acknowledgments

Received 7/21/2006; revised 11/24/2006; accepted 12/5/2006.

Grant support: National Cancer Institute of Canada using funds raised by the Terry Fox Run.

The costs of publication of this article were defrayed in part by the payment of page charges. This article must therefore be hereby marked *advertisement* in accordance with 18 U.S.C. Section 1734 solely to indicate this fact.

We thank Andrew Morrisson, May Cheung, and Pinjiang Cao for excellent technical help and Dr. Richard Hill for his critical comments.

References

1. Roos-Mattjus P, Sistonen L. The ubiquitin-proteasome pathway. Ann Med 2004;36:285–95.
2. Adams J. The proteasome: a suitable antineoplastic target. Nat Rev Cancer 2004;4:349–60.
3. Park DJ, Lenz HJ. The role of proteasome inhibitors in solid tumors. Ann Med 2004;36:296–303.
4. Bardos JI, Ashcroft M. Negative and positive regulation of HIF-1: a complex network. Biochim Biophys Acta 2005;1755:107–20.
5. Brahimi-Horn C, Mazure N, Pouyssegur J. Signalling via the hypoxia-inducible factor-1α requires multiple posttranslational modifications. Cell Signal 2005;17:1–9.
6. Semenza G. Signal transduction to hypoxia-inducible factor 1. Biochem Pharmacol 2002;64:993–8.
7. Salceda S, Caro J. Hypoxia-inducible factor 1α (HIF-1α) protein is rapidly degraded by the ubiquitin-proteasome system under normoxic conditions. Its stabilization by hypoxia depends on redox-induced changes. J Biol Chem 1997;272:22642–7.
8. Kallio PJ, Wilson WJ, O'Brien S, Makino Y, Poellinger L. Regulation of the hypoxia-inducible transcription factor 1α by the ubiquitin-proteasome pathway. J Biol Chem 1999;274:6519–25.
9. Mackay H, Hedley D, Major P, et al. A phase II trial with pharmacodynamic endpoints of the proteasome inhibitor bortezomib in patients with metastatic colorectal cancer. Clin Cancer Res 2005;11:5526–33.
10. Knowles HJ, Mole DR, Ratcliffe PJ, Harris AL. Normoxic stabilization of hypoxia-inducible factor-1α by modulation of the labile iron pool in differentiating

U937 macrophages: effect of natural resistance-associated macrophage protein 1. Cancer Res 2006;66:2600–7.
11. Knowles HJ, Tian YM, Mole DR, Harris AL. Novel mechanism of action for hydralazine: induction of hypoxia-inducible factor-1α, vascular endothelial growth factor, and angiogenesis by inhibition of prolyl hydroxylases. Circ Res 2004;95:162–9.
12. Vukovic V, Haugland HK, Nicklee T, Morrison AJ, Hedley DW. Hypoxia-inducible factor-1α is an intrinsic marker for hypoxia in cervical cancer xenografts. Cancer Res 2001;61:7394–8.
13. Hagg M, Wennstrom S. Activation of hypoxia-induced transcription in normoxia. Exp Cell Res 2005; 306:180–91.
14. Nakayama K, Frew IJ, Hagensen M, et al. Siah2 regulates stability of prolyl-hydroxylases, controls HIF1α abundance, and modulates physiological responses to hypoxia. Cell 2004;117:941–52.
15. Metzen E, Berchner-Pfannschmidt U, Stengel P, et al. Intracellular localisation of human HIF-1 α hydroxylases: implications for oxygen sensing. J Cell Sci 2003; 116:1319–26.
16. Mahon PC, Hirota K, Semenza GL. FIH-1: a novel protein that interacts with HIF-1α and VHL to mediate repression of HIF-1 transcriptional activity. Genes Dev 2001;15:2675–86.
17. Hon WC, Wilson MI, Harlos K, et al. Structural basis for the recognition of hydroxyproline in HIF-1α by pVHL. Nature 2002;417:975–8.
18. Min JH, Yang H, Ivan M, Gertler F, Kaelin WG, Jr., Pavletich NP. Structure of an HIF-1α-pVHL complex: hydroxyproline recognition in signaling. Science 2002; 296:1886–9.
19. Hirsila M, Koivunen P, Xu L, Seeley T, Kivirikko KI, Myllyharju Jl. Effect of desferrioxamine and metals on the hydroxylases in the oxygen sensing pathway. FASEB J 2005;19:1308–10.
20. Blagosklonny MV, An WG, Romanova LY, Trepel J, Fojo T, Neckers L. p53 inhibits hypoxia-inducible factor-stimulated transcription. J Biol Chem 1998;273: 11995–8.
21. Ravi R, Mookerjee B, Bhujwalla ZM, et al. Regulation of tumor angiogenesis by p53-induced degradation of hypoxia-inducible factor 1α. Genes Dev 2000;14:34–44.
22. Schmid T, Zhou J, Kohl R, Brune B. p300 relieves p53-evoked transcriptional repression of hypoxia-inducible factor-1 (HIF-1). Biochem J 2004;380:289–95.
23. Nieminen AL, Qanungo S, Schneider EA, Jiang BH, Agani FH. Mdm2 and HIF-1α interaction in tumor cells during hypoxia. J Cell Physiol 2005;204:364–9.
24. Hougardy BM, Maduro JH, van der Zee AG, et al. Proteasome inhibitor MG132 sensitizes HPV-positive human cervical cancer cells to rhTRAIL-induced apoptosis. Int J Cancer 2006;118:1892–900.
25. Latonen L, Kurki S, Pitkanen K, Laiho M. p53 and MDM2 are regulated by PI-3-kinases on multiple levels under stress induced by UV radiation and proteasome dysfunction. Cell Signal 2003;15:95–102.
26. Meng AX, Jalali F, Cuddihy A, et al. Hypoxia down-regulates DNA double strand break repair gene expression in prostate cancer cells. Radiother Oncol 2005;76: 168–76.
27. Semenza G. Targeting HIF-1 for cancer therapy. Nat Rev Cancer 2003;3:721–32.
28. Brahimi-Horn C, Pouyssegur J. When hypoxia signalling meets the ubiquitin-proteasomal pathway, new targets for cancer therapy. Crit Rev Oncol Hematol 2005; 53:115–23.
29. Sunwoo JB, Chen Z, Dong G, et al. Novel proteasome inhibitor PS-341 inhibits activation of nuclear factor-κB, cell survival, tumor growth, and angiogenesis in squamous cell carcinoma. Clin Cancer Res 2001;7:1419–28.
30. Nawrocki ST, Bruns CJ, Harbison MT, et al. Effects of the proteasome inhibitor PS-341 on apoptosis and angiogenesis in orthotopic human pancreatic tumor xenografts. Mol Cancer Ther 2002;1:1243–53.
31. Williams S, Pettaway C, Song R, Papandreou C, Logothetis C, McConkey DJ. Differential effects of the proteasome inhibitor bortezomib on apoptosis and angiogenesis in human prostate tumor xenografts. Mol Cancer Ther 2003;2:835–43.
32. Bruick RK, McKnight SL. A conserved family of prolyl-4-hydroxylases that modify HIF. Science 2001;294: 1337–40.
33. Epstein AC, Gleadle JM, McNeill LA, et al. C. elegans EGL-9 and mammalian homologs define a family of dioxygenases that regulate HIF by prolyl hydroxylation. Cell 2001;107:43–54.
34. Hirsila M, Koivunen P, Gunzler V, Kivirikko KI, Myllyharju J. Characterization of the human prolyl 4-hydroxylases that modify the hypoxia-inducible factor. J Biol Chem 2003;278:30772–80.
35. Safran M, Kaelin WG, Jr. HIF hydroxylation and the mammalian oxygen-sensing pathway. J Clin Invest 2003; 111:779–83.
36. Schofield CJ, Ratcliffe PJ. Oxygen sensing by HIF hydroxylases. Nat Rev Mol Cell Biol 2004;5:343–54.
37. Tuckerman JR, Zhao Y, Hewitson KS, et al. Determination and comparison of specific activity of the HIF-prolyl hydroxylases. FEBS Lett 2004;576:145–50.
38. Marxsen JH, Stengel P, Doege K, et al. Hypoxia-inducible factor-1 (HIF-1) promotes its degradation by induction of HIF-α-prolyl-4-hydroxylases. Biochem J 2004;381:761–7.
39. Chan DA, Sutphin PD, Denko NC, Giaccia AJ. Role of prolyl hydroxylation in oncogenically stabilized hypoxia-inducible factor-1α. J Biol Chem 2002;277:40112–7.
40. Appelhoff RJ, Tian YM, Raval RR, et al. Differential function of the prolyl hydroxylases PHD1, PHD2, and PHD3 in the regulation of hypoxia-inducible factor. J Biol Chem 2004;279:38458–65.
41. Berra E, Benizri E, Ginouves A, Volmat V, Roux D, Pouyssegur J. HIF prolyl-hydroxylase 2 is the key oxygen sensor setting low steady-state levels of HIF-1α in normoxia. EMBO J 2003;22:4082–90.
42. D'Angelo G, Duplan E, Boyer N, Vigne P, Frelin C. Hypoxia up-regulates prolyl hydroxylase activity: a feedback mechanism that limits HIF-1 responses during reoxygenation. J Biol Chem 2003;278:38183–7.
43. Aprelikova O, Chandramouli GV, Wood M, et al. Regulation of HIF prolyl hydroxylases by hypoxia-inducible factors. J Cell Biochem 2004;92:491–501.
44. Baek JH, Mahon PC, Oh J, et al. OS-9 interacts with hypoxia-inducible factor 1α and prolyl hydroxylases to promote oxygen-dependent degradation of HIF-1α. Mol Cell 2005;17:503–12.
45. Temes E, Martin-Puig S, Acosta-Iborra B, et al. Activation of HIF-prolyl hydroxylases by R59949, an inhibitor of the diacylglycerol kinase. J Biol Chem 2005;280:24238–44.
46. Lando D, Peet DJ, Gorman JJ, et al. FIH-1 is an asparaginyl hydroxylase enzyme that regulates the transcriptional activity of hypoxia-inducible factor. Genes Dev 2002;16:1466–71.
47. Jeong JW, Bae MK, Ahn MY, et al. Regulation and destabilization of HIF-1α by ARD1-mediated acetylation. Cell 2002;111:709–20.
48. Demidenko ZN, Rapisarda A, Garayoa M, Giannakakou P, Melillo G, Blagosklonny MV. Accumulation of hypoxia-inducible factor-1α is limited by transcription-dependent depletion. Oncogene 2005;24:4829–38.
49. Ema M, Hirota K, Mimura J, et al. Molecular mechanisms of transcription activation by HLF and HIF1α in response to hypoxia: their stabilization and redox signal-induced interaction with CBP/p300. EMBO J 1999;18:1905–14.
50. Kaluz S, Kaluzova M, Stanbridge EJ. Proteasomal inhibition attenuates transcriptional activity of hypoxia-inducible factor 1 (HIF-1) via specific effect on the HIF-1α C-terminal activation domain. Mol Cell Biol 2006;26: 5895–907.

Suppression of the Hypoxia-Inducible Factor-1 Response in Cervical Carcinoma Xenografts by Proteasome Inhibitors

Diana C. Birle and David W. Hedley

Cancer Res 2007;67:1735-1743.